Serdica J. Computing **6** (2012), 185–194

Serdica
Journal of Computing

Bulgarian Academy of Sciences
Institute of Mathematics and Informatics

TIME–HARMONIC BEHAVIOUR OF A CRACKED PIEZOELECTRIC SOLID BY BIEM*

Marin Marinov, Tsviatko Rangelov

Abstract. Time–harmonic behaviour of a cracked piezoelectric finite solid is studied by nonhypersingular traction Boundary Integral Equation Method (BIEM). A numerical solution for Crack Opening Displacement (COD) and Stress Intensity Factor (SIF) is obtained by using Mathematica. Several examples are presented to demonstrate the dependence of the solution on the crack position.

1. Introduction. Piezoelectric materials (PEM) have wide applications in transducers, actuators, wave generators and other smart intelligent systems. Due to their brittle structure and under dynamic load in service cracks appear and can cause their failure. Mathematical modeling of PEM with internal cracks leads to complicated boundary value problems (BVP) that have to be solved numerically in order to evaluate the wave field and especially its behaviour near the crack edges. Recently a number of results about the fracture behaviour of the

ACM Computing Classification System (1998): J.2, G.1.9

Key words: Piezoelectric finite solid, Anti-plane cracks, BIEM, SIF.

*The authors acknowledge the support of the Bulgarian NSF under the Grant No. DID 02/15.

piezoelectric solids were reported in the literature. Mostly infinite—piezoelectric domains are considered, see Shindo and Ozawa [11], Wang and Meguid [15], Narita and Shindo [9], Chen and Yu [2], Davi and Milazzo [3] where the BVP is transformed to dual integral equations and SIF is obtained as a solution of suitable Fredholm integral equations of a second type. For the investigations in a finite cracked domains, where the influence of the external boundary is taken into account, BIEM is a powerful tool, see Gross et al. [5], Dineva et al. [4], Rangelov et al. [10], Sladek et al. [12].

The aim of the work is to solve the BVP for anti–plane linear cracks in a finite PEM solid under time–harmonic mechanical and/or electrical load. The BVP is transformed to an equivalent integro–differential equation on the crack and on the external boundary. For the numerical solution Mathematica code is created and numerical examples are presented for different crack positions. The presented results have been reported partially in Marinov and Rangelov [7].

2. Boundary value problem. In a Cartesian coordinate system Ox in R^3 consider a finite transversally isotropic piezoelectric solid $\Omega \in R^2$, with boundary S and poled in Ox_3 direction. Let $\Gamma = \Gamma^+ \cup \Gamma^-$, $\Gamma \subset \Omega$ is an internal linear crack—an open segment. Assume that Ω is subjected to anti–plane mechanical and in–plane electrical time–harmonic load. The only non–vanishing displacements are the anti–plane mechanical displacement $u_3(x,t)$ and in–plane electrical displacement $D_i(x,t), i = 1,2,\ x = (x_1, x_2)$. Since all fields are time–harmonic with frequency ω the common multiplier $e^{i\omega t}$ is suppressed here and in the following. Assuming quasi-static approximation of piezoelectricity, the field equation in absence of body forces and electric charges is given by the balance equations

$$\sigma_{i3,i} + \rho\omega^2 u_3 = 0, \quad D_{i,i} = 0, \tag{1}$$

where the summation convention over repeated indices is applied. The strain–displacement and electric field–potential relations are

$$s_{i3} = u_{3,i}, \quad E_i = -\Phi_{,i}, \tag{2}$$

and the constitutive relations, see Landau and Lifshitz [6] are

$$\begin{aligned} \sigma_{i3} &= c_{44} s_{i3} - e_{15} E_i, \\ D_i &= e_{15} s_{i3} + \varepsilon_{11} E_i. \end{aligned} \tag{3}$$

where subscript $i = 1,2$ and comma denotes partial differentiation. Here σ_{i3}, s_{i3}, E_i, Φ are the stress tensor, strain tensor, electric field vector and electric potential,

respectively. Furthermore, $\rho > 0$, $c_{44} > 0$, e_{15}, $\varepsilon_{11} > 0$ are mass density, the shear stiffness, piezoelectric and dielectric permittivity characteristics. Introducing (3) and (2) into (1) leads to the coupled system

$$\begin{aligned} &c_{44}\Delta u_3 + e_{15}\Delta\Phi + \rho\omega^2 u_3 = 0, \\ &e_{15}\Delta u_3 - \varepsilon_{11}\Delta\Phi = 0. \end{aligned} \tag{4}$$

where Δ is the Laplace operator. The basic equations (3), (4) can be written in a more compact form if the notation $u_J = (u_3, \Phi)$, $J = 3, 4$ is introduced. The constitutive equations (3) then take the form

$$\sigma_{iJ} = C_{iJKl} u_{K,l}, \quad i, l = 1, 2, \tag{5}$$

where $C_{i33l} = \begin{cases} c_{44}, i = l \\ 0, \quad i \neq l \end{cases}$, $C_{i34l} = C_{i43l} = \begin{cases} e_{15}, i = l \\ 0, \quad i \neq l \end{cases}$, $C_{i44l} = \begin{cases} -\varepsilon_{11}, i = l \\ 0, \qquad i \neq l \end{cases}$
and system (4) is reduced to

$$L(u) \equiv \sigma_{iJ,i} + \rho_{JK}\omega^2 u_K = 0, \quad J, K = 3, 4, \tag{6}$$

where $\rho_{JK} = \begin{cases} \rho, J = K = 3 \\ 0, J = 4 \text{ or } K = 4 \end{cases}$.

The boundary conditions on the outer boundary S are given as a prescribed traction $\bar{t}_J$

$$t_J = \bar{t}_J \ \text{ on } S, \tag{7}$$

where $t_J = \sigma_{iJ} n_i$ and $n = (n_1, n_2)$ is the outer normal vector. The boundary condition along the crack is

$$t_J = 0 \ \text{ on } \Gamma^+ \tag{8}$$

and this means that the crack is free of mechanical traction as well as of surface charge, i.e. the crack is electrically impermeable.

Following Akamatsu and Nakamura [1] it can be proved that the BVP (6)–(8) admits a continuously differentiable solution if the usual smoothness and compatibility requirements for the boundary data are satisfied. Consider the following BVPs:

$$\left| \begin{aligned} &L(u^1) = 0 \quad \text{in } \Omega, \\ &t_J^1 = \bar{t}_J \quad \text{on } S, \end{aligned} \right. \tag{9}$$

$$\left|\begin{array}{l} L(u^2)=0 \quad \text{in } \Omega\backslash\Gamma, \\ t_J^2=-t_J^1 \quad \text{on } \Gamma^+ \\ t_J^2=0 \quad \text{on } S. \end{array}\right. \tag{10}$$

Since BVP (6)–(8) is linear, its solution is a superposition of BVPs (9), (10), so $u_J = u_J^1 + u_J^2$ and $t_J = t_J^1 + t_J^2$. The fields u_J^1, t_J^1 are obtained by the dynamic load on S in the crack free domain Ω, while u_J^2, t_J^2 are produced by the load $t^2 = -t_J^1$ on Γ^+ and zero boundary conditions on S.

3. Non–hypersingular BIEM. Following Wang and Zhang [14], Rangelov et al. [10] the system of BVPs (9), (10) is transformed to an equivalent system of integro–differential equations on $S \cup \Gamma$.

$$\begin{aligned} &\frac{1}{2}t_J^1(x) = C_{iJKl}n_i(x)\int_S [(\sigma^*_{\eta PK}(x,y)u^1_{P,\eta}(y) - \rho_{QP}\omega^2 u^*_{QK}(x,y)u^1_P(y))\delta_{\lambda l} \\ &-\sigma^*_{\lambda PK}(x,y)u^1_{P,l}(y)]n_\lambda(y)dS - C_{iJKl}n_i(x)\int_S u^*_{PK,l}(x,y)t^1_P(y)dS, \quad x\in S, \end{aligned} \tag{11}$$

$$\begin{aligned} &t_J^c(x) = C_{iJKl}n_i(x)\int_{\Gamma^+} [(\sigma^*_{\eta PK}(x,y)\Delta u^2_{P,\eta}(y) \\ &-\rho_{QP}\omega^2 u^*_{QK}(x,y)\Delta u^2_P(y))\delta_{\lambda l} - \sigma^*_{\lambda PK}(x,y)\Delta u^2_{P,l}(y)]n_\lambda(y)d\Gamma \\ &+C_{iJKl}n_i(x)\int_S [(\sigma^*_{\eta PK}(x,y)u^2_{P,\eta}(y) - \rho_{QP}\omega^2 u^*_{QK}(x,y)u^2_P(y))\delta_{\lambda l} \\ &-\sigma^*_{\lambda PK}(x,y)u^2_{P,l}(y)]n_\lambda(y)dS, \quad x\in S\cup\Gamma. \end{aligned} \tag{12}$$

Here $t_J^c(x) = \begin{cases} -t_J^1(x), & x\in\Gamma^+ \\ t_J^2(x), & x\in S \end{cases}$, u^*_{JK} is the fundamental solution of Eq. (6), $\sigma^*_{iJQ} = C_{iJKl}u^*_{KQ,l}$ is the corresponding stress, and $\Delta u_J^2 = u_J^2|_{\Gamma^+} - u_J^2|_{\Gamma^-}$ is the generalized COD on the crack Γ, $x=(x_1,x_2)$ and $y=(y_1,y_2)$ denote the position vector of the observation and source point, respectively. The functions $u_J, t_J, u^*_{JK}, \sigma_{iJQ}$ additionally depend on the frequency ω, which is omitted in the list of arguments for simplicity. Equations (11), (12) constitute a system of integro–differential equations for the unknown Δu_J^2 on the line Γ, t_J^1 on Γ^+ and u_J^1, u_J^2 on the external boundary of the piezoelectric solid. From its solution the generalized displacement u_J at every internal point of G can be determined by using the corresponding representation formulae, see Wang and Zhang [14] and Gross et al. [5].

In order to solve the system (11), (12) it is necessary to know the fundamental solution u^*_{JK} and corresponding stress σ^*_{lQK} in a closed form. The fundamental solution of Eq. (6) is defined as the solution of the equation

$$\sigma^*_{iJM,i} + \rho_{JK}\omega^2 u^*_{KM} = -\delta_{JM}\delta(x,\xi), \tag{13}$$

where δ is the Dirac distribution, x, ξ are source and field points respectively and δ_{JM} is the Kronecker symbol. The fundamental solution for piezoelectric solids under anti–plane mechanical and in–plane electrical loading is derived in Rangelov et al. [10] using the Radon transform, see also Marinov and Rangelov [8].

4. Numerical solution. The numerical procedure for the solution of the boundary value problem follows the numerical algorithm developed and validated in Rangelov et al. [10] and Dineva et al. [4]. The outer boundary S and the crack Γ are discretized by quadratic boundary elements (BE). In order to model the correct asymptotic behavior of the displacement (like $\sqrt{r}$) and the traction (like $1/\sqrt{r}$) near the crack tips a special crack–tip quarter–point BE is used. Applying the shifted point scheme, the singular integrals converge in Cauchy principal value (CPV) sense, since the smoothness requirements of the approximation $\Delta u_J \in C^{1+\alpha}(\Gamma)$ are fulfilled. Due to the form of the fundamental solution as an integral over the unit circle, all integrals in (11), (12) are two-dimensional. In general there appear two types of integrals–regular integrals and singular integrals, the latter including a weak "$\ln r$" type singularity and also a strong "$\frac{1}{r}$" type singularity. The regular integrals are solved using a Quasi-Monte Carlo method, while the singular integrals are solved with a combined method–partially analytically as CPV integrals. After the discretization procedure an algebraic linear complex system of equations is obtained and solved.

The program code based on Mathematica 8 has been created following the procedure outlined above.

The mechanical dynamic SIF K_{III}, the electrical displacement intensity factor K_D and the electric intensity factor K_E are obtained directly from the traction nodal values ahead of the crack-tip, see Suo et al. [13]. In a local polar coordinate system (r, φ) with the origin the crack edge the formulae are

$$
\begin{aligned}
&K_{III} = \lim_{r\to\pm 0} t_3\sqrt{2\pi r}, \quad K_D = \lim_{r\to\pm 0} t_4\sqrt{2\pi r},\\
&K_E = \lim_{r\to\pm 0} E_3\sqrt{2\pi r}, \quad E_3 = \frac{1}{e_{15}^2 + c_{44}\varepsilon_{11}}(-e_{15}t_3 + c_{44}t_4),
\end{aligned}
\tag{14}
$$

where t_J is the generalized traction at the point (r, φ) close to the crack-tip.

The Mathematic's code consists of the following parts:

(i) Definition of the material parameters, S and Γ geometry, BE and quadratic approximation;

(ii) Definition of the fundamental solution, its derivatives and the asymptotic for small arguments;

(iii) Definition of the integro–differential equations (11), (12) and the anti–plane load;

(iv) Solution of the integrals and forming the system of linear equations for the unknowns $u_J^1, t_J^1, \Delta u_J^2$;

(v) Solution of the linear system;

(vi) Formulae for the solution in every point of Ω;

(vii) Evaluation of the SIF–the leading coefficients in the asymptotic of the solution near the crack edges.

The main points in the solution procedure are (iv) and (v). In (iv) the integrals over the BE are two-dimensional (in the intrinsic coordinates in the domain $(z, \varphi) \in [-1, 1] \times [0, 2\pi]$) with regular and singular kernels: with weak singularity as $O(\log r)$ and with strong singularities $O(1/r)$. The regular integrals are solve a using the AdaptiveMonteCarlo Method with 300 points. The singular integrals are solved analytically with respect to r and numerically with respect to φ, see Dineva et al. [4]. The difficulties in (v) (due to the fact that the material parameters vary in the rate of 10^{10}: for mechanical stiffness c_{44}, 10 for the piezoelectric parameter e_{15} and for the dielectric parameters ε_{11} in the rate of 10^{-10}) are resolved using functions Solve or FindInstance.

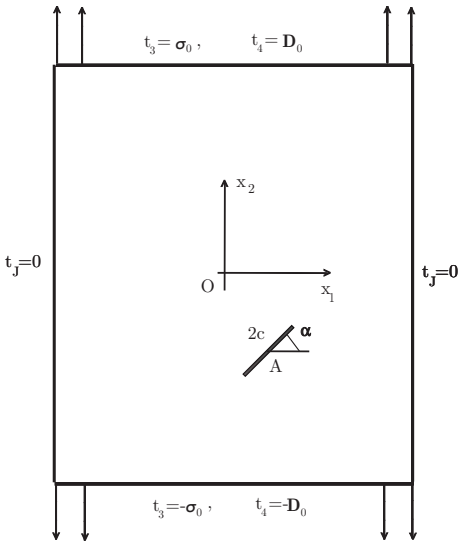

Fig. 1. Cracked rectangular finite solid

5. Numerical results. The material used in the numerical examples is PZT-4, whose data are $c_{44}^0 = 2.56 \times 10^{10}$ N/m^2, $e_{15}^0 = 12.7$ C/m^2, $\varepsilon_{11}^0 = 64.6 \times 10^{-10}$ C/Vm and $\rho^0 = 7.5 \times 10^3$ kg/m^3. The length of the linear crack Γ is $2c = 5$ mm, while the rectangular domain Ω has dimension 20 mm$\times$40 mm. The crack is inclined with angle α with respect to the Ox_1 axis and its center is at the point $A(a_1, a_2)$. It is discretized by 7 BE with lengths l_j: $l_1 = l_7 = 0.375$ mm, $l_2 = l_6 = 0.5$ mm, $l_3 = l_5 = 1.0$ mm, $l_4 = 1.25$ mm. The boundary S is discretized by 20 BE. The time–harmonic load is uniform electromechanical tension in Ox_2 direction with amplitudes $\sigma_0 = 400 \times 10^6$N/m^2 and $D_0 = 10^{-5}$C/m^2, see Figure 1.

Validation of the numerical code for the finite solid Ω is done using truncation

method. The problem (11), (12) is solved in the center cracked square Ω_a with a side $2a$ with $a > 10c$. In this case the outer boundary S_a does not influence the result significantly in the considered frequency range and a comparison of the SIF with those in in Wang and Meguid [15] for the cracked plane gives good coincidence, see Dineva et al. [4].

In the presented examples the normalized frequency is $\Omega = c\sqrt{\rho^0/(c_{44} + \dfrac{e_{15}^2}{\varepsilon_{11}})}\omega$. In the figures there are plotted the absolute values of the normalized SIFs $K_{III}^* = \dfrac{K_{III}}{\sigma_0\sqrt{\pi c}}$ and $K_E^* = \dfrac{K_E}{\sigma_0\sqrt{\pi c}}$.

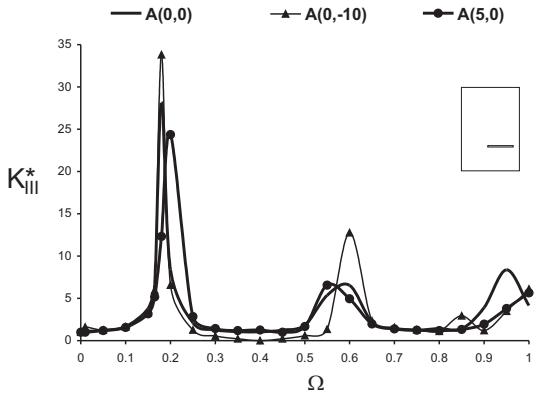

Fig. 2. Normalized mechanical SIF versus normalized frequency under electromechanical load with amplitudes $\sigma_0 = 400 \times 10^6$ N/m^2, $D_0 = 10^{-5}$ C/m^2 for different crack positions with center A in mm and angle $\alpha = 0$

In Figure 2 the BIEM solution for K_{III}^* versus $\Omega \in (0, 1.0)$ is given for different crack positions with $\alpha = 0$. It is observed that the first peak is around $\Omega = 0.18$, which corresponds to resonance frequency of the considered BVP and shows the influence of the boundary S on the SIF. The second peak is around 0.6 and the third peak is around 0.95. The peak–value depends on the crack position–the highest value of 33.8 is for the case of $A(0, -10)$–the crack is close to the lower boundary. Note that in the truncation domain the peak is around $\Omega = 0.71$ and its value is 1.31 with comparison with the peak of 28.11 for crack with center $A(0, 0)$ in the finite domain.

Figure 3 presents the dependence of SIFs K_{III}^* and K_E^* for fixed normalized frequency $\Omega = 0.2$ on the position of the crack with center at the origin and inclined with angle $\alpha = \dfrac{\pi}{10}k$, $k = 0, \ldots, 5$ with respect to Ox_1 axis. Due to the

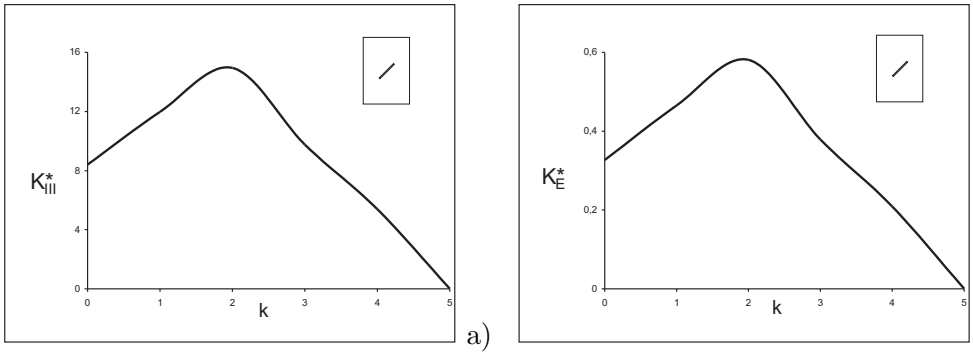

a) b)

Fig. 3. Normalized SIFs versus inclined crack angle $\alpha = \frac{\pi}{10}k$, $k = 0, \ldots, 5$ at normalized frequency $\Omega = 0.2$ and under electromechanical load with amplitudes $\sigma_0 = 400 \times 10^6$ N/m^2, $D_0 = 10^{-5}$ C/m^2: a) K^*_{III}, b) K^*_E

symmetry of the crack with respect to the applied load, SIFs in the left and right crack–tips are equal. The maximum values are for $k \in (2, 3)$, around $\alpha = \dfrac{\pi}{6}$ while for a crack parallel to the direction of the applied tension, i.e. $\alpha = \dfrac{\pi}{2}$, both SIFs are zero.

Figure 4 shows SIF K^*_{III} versus the normalized frequency $\Omega \in (0, 1.0)$ for different crack's inclined angles $\alpha = 0, \pi/3, \pi/4, \pi/6$ and crack's center $A(0, 0)$. The maximum value of SIF is for $\alpha = 0$ and with α increasing the peaks of the SIF decreases.

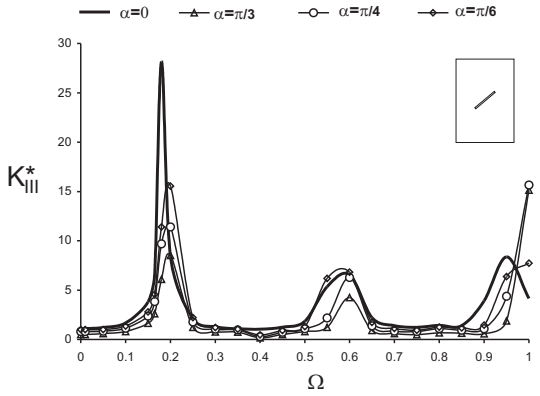

Fig. 4. Normalized mechanical SIF versus normalized frequency for different angles α of the inclined crack with center $A(0, 0)$

6. Conclusion. The time–harmonic anti–plane crack problem for piezoelectric finite solid is solved numerically by means of non–hypersingular traction BIEM and Mathematica code is developed. Numerical examples for SIF computation are presented and analyzed. The proposed numerical solution and program code can be applied for solution of crack interaction problems in finite PEM as well as for solution of the corresponding inverse problems.

REFERENCES

[1] Akamatsu M., G. Nakamura. Well-posedness of initial-boundary value problems for piezoelectric equations. *Applicable Analysis*, **81** (2002), 129–141.

[2] Chen Z., S. Yu. Anti–plane vibration of cracked piezoelectric materials. *Mech. Res. Commun.*, **25** (1998), No 3, 321–327.

[3] Davi G., A. Milazzo. Multi-domain boundary integral formulations for piezoelectric materials fracture mechanics. *Int. J. Solids Str.*, **38** (2001), 7065–7078.

[4] Dineva P., D. Gross, R. Müller, T. Rangelov. BIEM analysis of dynamically loaded anti-plane cracks in graded piezoelectric finite solids. *Int. J. Solids Str.*, **47** (2010), 3150–3165.

[5] Gross D., P. Dineva, T. Rangelov. BIEM solution of piezoelectric cracked finite solids under time-harmonic loading. *Eng. Anal. Bound. Elem.*, **31** (2007), No 2, 152–162.

[6] Landau D. L., E. M. Lifshitz. Electrodynamics of Continuous Media. Pergamon Press, Oxford, 1960.

[7] Marinov M., T. Rangelov. BIEM solution for cracked finite piezoelectric solids using Mathematica. In: Proceedings of 7 ICCSE 2011 (Eds R. Stainov, V. Kanabar, P. Assenova), 224–239.

[8] Marinov M., T. Rangelov. Integro–differential equations for anti–plane cracks in inhomogeneous piezoelectric plane. *Comptes rendus Acad. Bulg. Sci.*, **64** (2011), No 12, 1669–1678.

[9] Narita F., Y. Shindo. Dynamic anti–plane shear of a cracked piezoelectric ceramics. *Theor. Appl. Mech.*, **29** (1998), 168–180.

[10] Rangelov T., P. Dineva, D. Gross. Effect of material inhomogeneity on the dynamic behaviour of cracked piezoelectric solids: a BIEM approach. *ZAMM - Z. Angew. Math. Mech.*, **88** (2008), No 2, 86–99.

[11] Shindo Y., E. Ozawa. Dynamic analysis of a cracked. Mechanical Modeling of New Electromagnetic Materials(Ed. R. K. T. Hsieh), Elsevier, 1990, 297–304.

[12] Sladek J., V. Sladek, Ch. Zhang, P. Solek, L. Starek. Fracture analysis in continuously nonhomogeneous piezoelectric solids by the MLPG. *Comput. Methods Eng. Sci.*, **19** (2007), No 3, 247–262.

[13] Suo Z., C. Kuo, D. Barnett, J. Willis. Fracture mechanics for piezoelectric ceramics. *J. Mech. Phys. Solids*, **40** (1992), 739–765.

[14] Wang C-Y., C. Zhang. 2D and 3D dynamic green's functions and time-domain bie formulations for piezoelectric solids. *Engng. Anal. BE*, **29** (2005), 454–465.

[15] Wang X. D., S. A. Meguid. Modelling and analysis of the dynamic behaviour of piezoelectric materials containing interfacing cracks. *Mech. Mater.*, **32** (2000), 723–737.

Marin Marinov
Computer Science Department
New Bulgarian University
1618 Sofia, Bulgaria
e-mail: mlmarinov@nbu.bg

Tsviatko Rangelov
Institute of Mathematics and Informatics
Bulgarian Academy of Sciences
1113 Sofia, Bulgaria
e-mail: rangelov@math.bas.bg

Received March 2, 2012
Final Accepted May 3, 2012